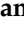





Article

Groundwater Quality Assessment Using Multi-Criteria GIS Modeling in Drylands: A Case Study at El-Farafra Oasis, Egyptian Western Desert

Hanaa A. Megahed¹, Hossam M. GabAllah¹, Rasha H. Ramadan², Mohamed A. E. AbdelRahman^{2,*}, Paola D'Antonio^{3,*}, Antonio Scopa³ and Mahmoud H. Darwish⁴

¹ Division of Geological Applications and Mineral Resources, National Authority for Remote Sensing and Space Sciences (NARSS), Cairo 1564, Egypt

² Division of Environmental Studies and Land Use, National Authority for Remote Sensing and Space Sciences (NARSS), Cairo 1564, Egypt

³ Scuola di Scienze Agrarie, Forestali, Alimentari ed Ambientali (SAFE), Università degli Studi della Basilicata, Viale dell'Ateneo Lucano, 10, 85100 Potenza, Italy

⁴ Geology Department, Faculty of Science, New Valley University, El Kharga 72511, Egypt

* Correspondence: maekaoud@narss.sci.eg (M.A.E.A.); paola.dantonio@unibas.it (P.D.)

Abstract: The most critical issue that was the main research interest is its groundwater quality which is vital for public health concerns. Groundwater is a significant worldwide water supply for diverse communities, especially in dryland regions. Groundwater quality assessment in desert systems is largely hindered by the lack of hydrological data and the remote location of desert Oases. This study provides a preliminary understanding of the influences of climate, land usage, and population growth on the groundwater quality in El-Farafra Oasis in the Western Desert in Egypt from 2000 to now. Therefore, the study's main objective was to determine the extent of change in temporal water quality and the factors causing it. The present study integrates chemical analyses and geospatial modeling better to assess groundwater quality in the study area. A chemical analysis of thirty-one groundwater samples from wells representing each study area was carried out during three time periods (2000, 2010, and 2022). Several chemical properties of groundwater samples gathered from wells in the research area were analyzed. Furthermore, the groundwater quality trend from 2000 to the present was identified using three approaches: Wilcox and Schoeller Diagram in Aq.QA software, interpolation in the ArcGIS software, and Ground Water Quality Index (GWQI). Moreover, the influence of changing land usage on groundwater quality was studied, and it was found that the increase in agriculture and urbanization areas is linked to groundwater quality degradation. The findings revealed that the barren area in 2000, 2010, and 2022 was 371.7, 362.0, and 343.2 km², respectively, which indicates a substantial decrease of 6.2% within this research timeframe. In contrast, agriculture and human-made structures have expanded by 1.8%. Also, population growth has led to an increase in water consumption as the population has grown at a rate of 7.52% annually from 2000 to 2020. As the climatic condition increases from 2000 to 2022, these changes could extend to the water quality in shallow aquifers with increasing evaporation. Based on the water quality spatial model, it is found that, despite a declining tendency in the rate of precipitation and an expansion in agricultural areas and population growth, the water quality was still appropriate for human and farming consumption in large areas of the study area. The presented approach is applicable to the assessment of groundwater in desert regions in the Middle East area.

Keywords: groundwater quality; population pressure; spatial model; climate change; land use; western desert; El-Farafra Oasis; Egypt



Citation: Megahed, H.A.; GabAllah, H.M.; Ramadan, R.H.; AbdelRahman, M.A.E.; D'Antonio, P.; Scopa, A.; Darwish, M.H. Groundwater Quality Assessment Using Multi-Criteria GIS Modeling in Drylands: A Case Study at El-Farafra Oasis, Egyptian Western Desert. *Water* **2023**, *15*, 1376. <https://doi.org/10.3390/w15071376>

Academic Editors: Dionysia Panagoulia and Domenico Cicchella

Received: 15 February 2023

Revised: 26 March 2023

Accepted: 27 March 2023

Published: 3 April 2023



Copyright: © 2023 by the authors. Licensee MDPI, Basel, Switzerland. This article is an open access article distributed under the terms and conditions of the Creative Commons Attribution (CC BY) license (<https://creativecommons.org/licenses/by/4.0/>).

1. Introduction

Groundwater (GW) is a significant resource of drinkable water, and about 45% or more of the water is employed for agricultural purposes for almost 50% of the planet's

inhabitants [1], which denotes a significant volume of freshwater taken from the world [2]. GW resources have been impacted by climatic and land use changes, which represent major stressors and an influence on the groundwater quality and quantity [3,4] and may influence hydrologic cycle like as evapotranspiration and surface infiltration, leading to changes in surface and subsurface flows [5–7]. Naturally, the chemical composition of the groundwater depends on multiple factors including; recharge water quality, earth materials types, water-soil-rock interaction, groundwater dynamics, and hydrogeological setup, etc. [8]. Among the influences that change the quality of groundwater are human activities and geological formations that carry water [9–11]. Surface and Groundwater pass through a complex cycle in the atmosphere, the earth's surface, and the soil [12].

Recently, our world is currently subjected to unprecedented climate changes leading to serious environmental issues [13]. Many researchers have conducted their studies to analyze and interpret the hydrological influences of climate and land usage changes [14–16]. For instance, increased global temperatures; lowered water resources' pH, and varying levels of global precipitation from greenhouse gas emissions (CO₂) are caused by human activities [17]. Several studies [3,18] showed that the causes of the groundwater quality changes and a drop in groundwater amounts were climate change, the overuse of fertilizers, and the conversion of forests to farming, which resulted in increased pollutants and usage of artificial nitrogen fertilizer. Many studies demonstrated that modifications in the vegetative ecosystem produced by alterations in land use and land cover substantially impacted the local hydrological cycle [19,20]. Subsequently, the component of land cover/land use changes within the catchment affecting the hydrological cycle seems crucial in advancing hydrology [21,22]. On the other hand, groundwater quality is greatly affected by the surrounding human activities, and therefore groundwater supplies and water quality can be influenced by population growth and increasing urbanization rate [23–25].

The alteration in land usage was correlated with information on water quality, and it was shown that the regions around fast urban growth and industry contain groundwater of poor to unfit quality [26]. The capability to conduct a spatial study of fluctuations in groundwater quality is vital in environmental managers' decision-making processes. Several research papers used satellite imagery, Remote Sensing (RS), and Geographic Information System (GIS) techniques to investigate the phenomenon of temporal and geographical variations in land usage [27–30], also WQI which has been successfully used in the assessment of water quality [31], as well as the connection between the quality of groundwater and variations in land cover/land use [3,32–35]. During 2001–2005, Houben et al. [36] investigated the quality of groundwater in Afghanistan's Kabul watershed. They discovered that due to the repeated droughts, this area experienced a rise in the salinity and hardness of its groundwater. In addition, Ketata et al. [37] examined the behavior of variation in some groundwater hydrochemical parameters from 1995 to 2003 in Gabès, Tunisia. They concluded that salt concentration and other chemical parameters in groundwater streamlines have diminished over time. Elci and Polat [38] focused on the behavior of water quality fluctuations in Turkey's Nife groundwater. They found that during rainy seasons, chloride concentrations were lower than during dry seasons.

Furthermore, investigations conducted in Iran revealed a worsening in the groundwater quality in Iran's plains from 1998 to 2004 [39]. An examination of temporal and geographical variations of groundwater status in the Qazvin plain from 2003 to 2007 revealed that groundwater quality decreased during rainy seasons, demonstrating the effect of rains on groundwater quality [40]. Based on the results of Singh et al. [41], owing to modifications in land cover and land use trends, natural and artificial recharge resulted in a rise in groundwater volume (increased area of fallow land). Fertilizers, conversely, degraded the groundwater quality. Singh et al. [41] resolved that the deterioration in groundwater quality in many agricultural areas, as well as those near urban and industrial areas, has heightened conservation concerns among many governmental organizations.

In semi-arid and arid regions, groundwater is an increasingly significant resource for irrigation, industrial, and drinking. Egypt is a country located in these arid zones, and as

a result of this geographic location, Egypt may be highly susceptible to climate change. In the current area under consideration, groundwater and springs remain a key source of fresh water for drinking and irrigation purposes. Many Egyptian studies considered the changes in hydrological, geological, and land use [42–44]. This research explores the alteration in groundwater quality in EL-Farafa Oasis and the association between its land use modification and climate change from 2000 to the present. The New Valley Project, which started in the 1960s, is pumping water from the famous Nubian Sandstone Aquifer (NSA) to the oasis of El Farafa in the Western Desert so that the desert may be farmed and restored [45]. Even though a large number of deep-water wells were constructed for this project, the issue became immediately obvious since it threatened the oasis's primary spring water source [46]. Land use changes and climate changes in the present work are being applied for the first time in the Egyptian Western Desert to evaluate their possible effects on groundwater quality. The present work is carried out to explore the following objectives: (i) using remote sensing and satellite photos to evaluate the previous and current land use changes and their effects in the study region from 2000 to the present, (ii) analyzing the water quality indices for the groundwater samples and mapping their spatial distributions using remote sensing and GIS models, and (iii) study the possible influences of change in climate and land use on groundwater quality.

2. Study Area Description

Geographically, El-Farafa Oasis is placed in the Egyptian Western Desert (EWD) between latitude and longitude; $26^{\circ}45'41''$ – $27^{\circ}13'40''$ N and $27^{\circ}42'51''$ – $27^{\circ}59'32''$ E (Figure 1). El-Farafa Oasis has a hot hyper-arid desert climate, with hot and dry summers marked by a lack of precipitation and moderate winters with intermittent precipitation and a yearly mean air temperature of 25°C [47]. Rainfall in the area is rare, with occasionally heavy rainfall in a short duration with yearly precipitation averaging below 10 mm [45].

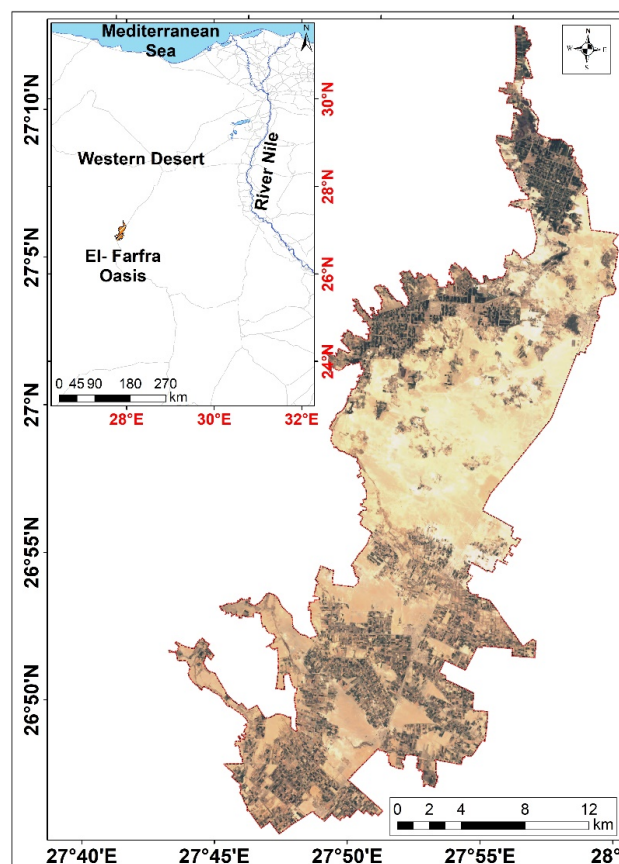


Figure 1. Location map of the study area (Landsat 8).

Geologically, the research area is covered with geologic rock formations that range in age from the Quaternary to the Upper Cretaceous. From top to bottom, the rock units are distinguished as follows: Quaternary deposits (containing sand sheets, sand dunes, and playa deposits), Tertiary formations (including Farafra limestone, Esna Shale, and Tarawan Chalk), and the Upper Cretaceous Khoman Formation. Upper Cretaceous to Pre-Cambrian geologic formations can be found in the subsurface. At the same time, the Upper Cretaceous and Paleozoic sediments that make up the Nubian Sandstone sequence are among the subsurface geological formations and are underlain by basement rocks [48] (Figure 2).

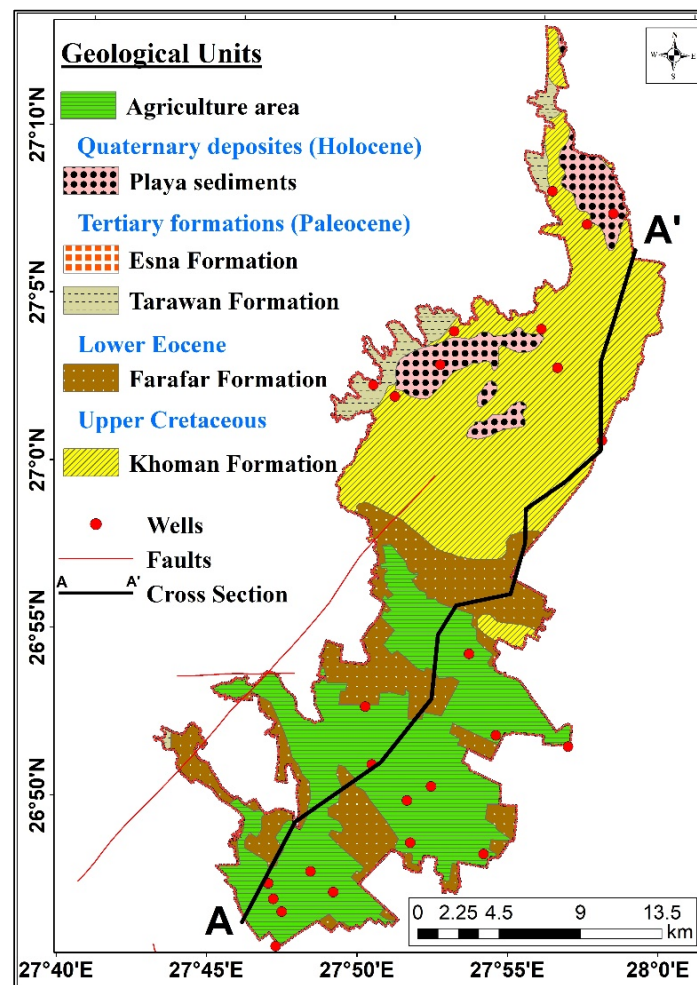


Figure 2. Geological map of the study area (modified by UNESCO, 2005).

From a hydrogeological perspective, the samples are collected from The Nubian Sandstone Aquifer System (NSAS) (confined aquifer) with an average well depth of 600 m. The Nubian Sandstone Aquifer System (NSAS) is composed of two hydrological units namely; the Nubian Aquifer System (NAS) and the Post Nubian Aquifer System (PNAS) that are separated by the upper Cretaceous aquitard of the Dakhla Formation [49]. The NAS outcrops south of latitudes 28° and then it becomes a confined aquifer to the north in El-Farafra Oasis (Figure 3) [50,51]. The NAS groundwater has been mainly recharged during the previous wet climatic periods during the Pleistocene with a very limited recharge during the present arid conditions [52]. The PNAS mainly receives recharge through vertical connection with the NAS along major geological structures [49]. Therefore, both aquifers receive negligible volumes of modern recharge and thus avoiding potential contamination from surface water sources [53].

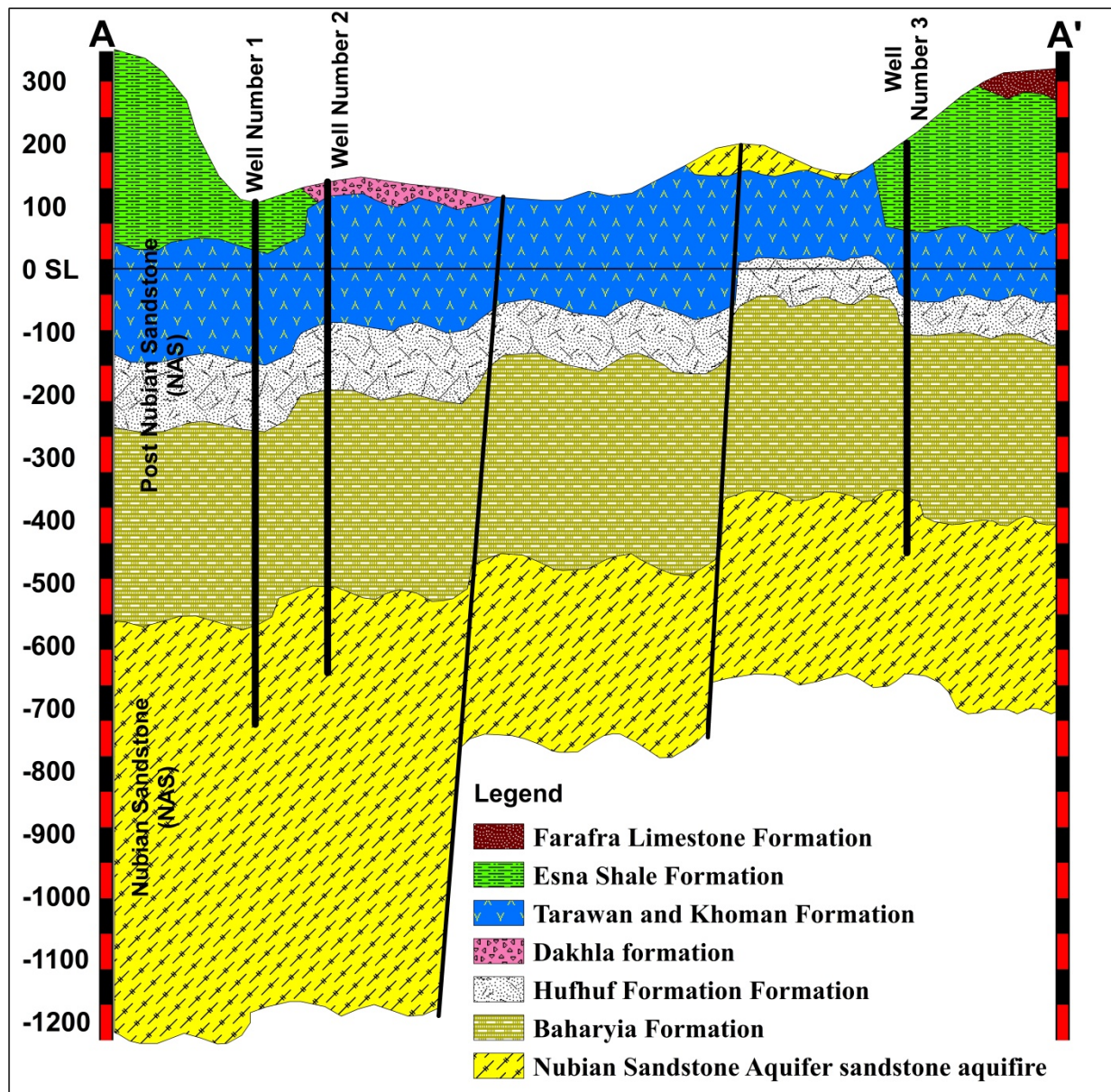


Figure 3. Hydrogeologic cross-section along SW-NE of the study area, (modified by UNESCO, 2005).

3. Materials and Methods

About 31 groundwater samples from the wells (Figure 4) were selected from all the wells in the study area (Figure 5). These selected wells were drilled before the year 2000 with different depths and water samples were taken during three time periods, 2000, 2010, and then 2022. Groundwater samples were collected in plastic containers for physical and chemical analysis. The physical parameters, pH, electrical conductivity, and dissolved solids were measured in the field by portable multiparametric devices. After about half an hour of pumping the wells, water samples were taken. All samples were sealed and kept until chemical analysis was carried out in the laboratory. Chemical analysis of the major cations and anions (Na^+ , K^+ , Ca^{2+} , Mg^{2+} , HCO_3^- , SO_4^{2-} , and Cl^-) was performed according to international standards. The flame photometer technique used to determine potassium and sodium, calcium, and magnesium was analyzed using atomic absorption spectrophotometer, Bicarbonate was determined by titration method, and sulfate and chloride were determined colorimetrically. Chemical analyses were carried out at the Central Water Laboratory in Kharga City. The chemical analysis results of the wells are given in

(Table 1). Various groundwater quality indices were produced in the present work using geographical information system (GIS) to assess and map changes in groundwater quality resulting from land use and climate alterations. Seven standard water quality indices were calculated. TDS, EC, SAR, SO_4^{2-} , and HCO_3^- refer to total dissolved solids, electrical conductivity, sulfate, and bicarbonates, respectively. The research used various approaches to examine variations in groundwater quality, including interpolation techniques for mapping the changes, Wilcox and Schoeller Diagrams for measuring quality in farming, and the GWQI index for assessing the quality of drinking water. Therefore, three methods are applied to investigate groundwater quality using spatially based GIS (IDW, ordinary kriging, and RBF). The linear technique of displaying the spatial distribution of the concentration of the parameters was utilized in the kriging method, which was used for most parameters because it has the least error [54–56]. Wilcox [57] and Schoeller's [58] diagrams have been employed to assess the quality of water for consumption and agricultural purposes, based on the water's ionic compositions and total soluble salts [59].

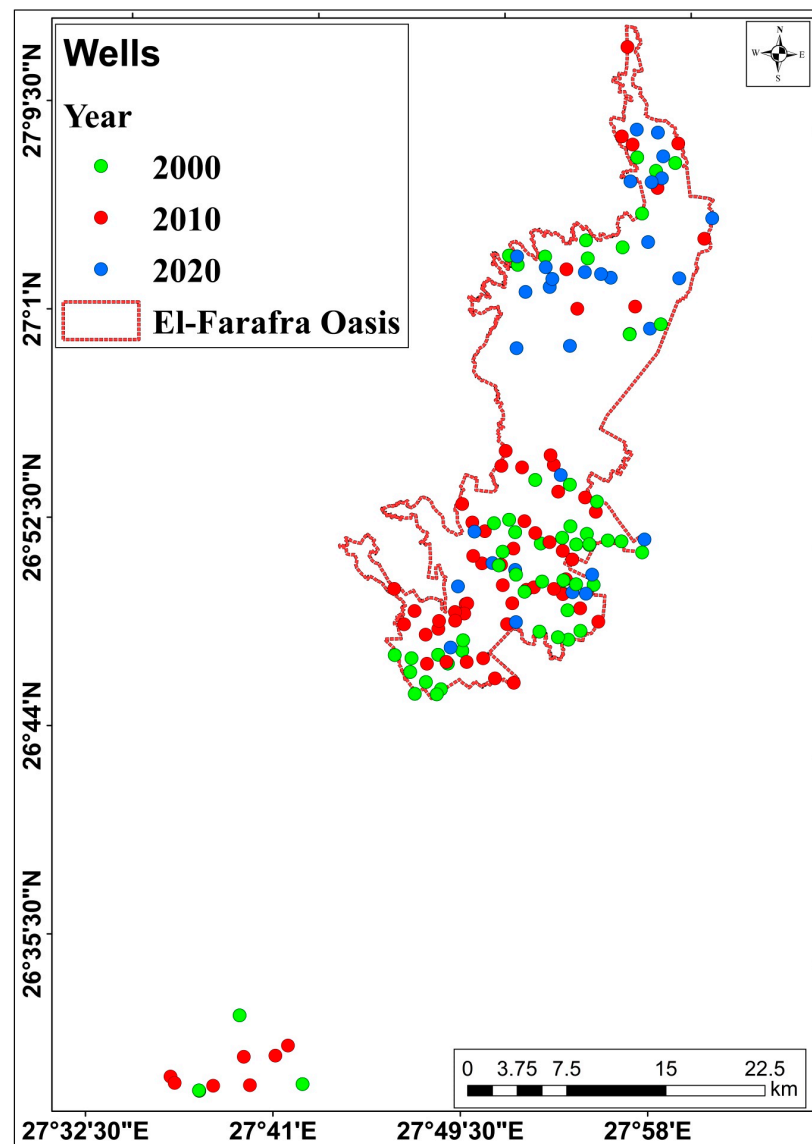


Figure 4. Location of the groundwater samples in the study area.

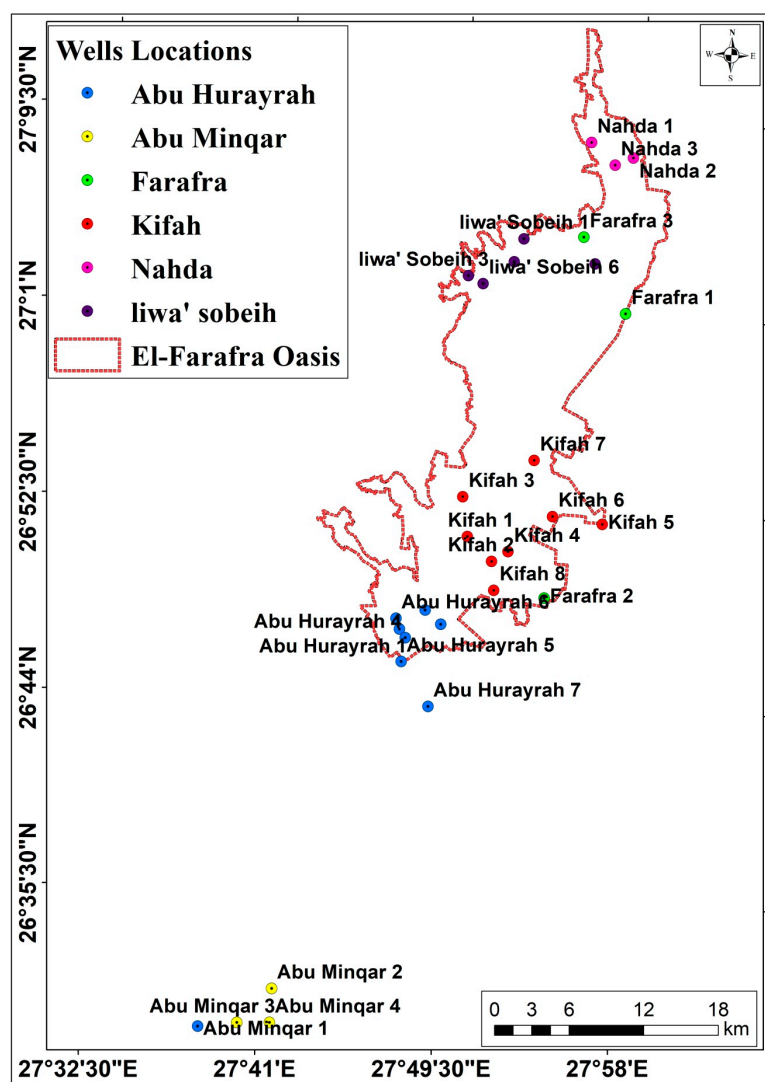


Figure 5. Location of the groundwater wells in the study area, (2022).

Table 1. Chemical analyses results of the groundwater samples.

Parameters		pH	TDS	Ca ²⁺	Mg ²⁺	Na ⁺	K ⁺	HCO ₃ ⁻	Cl ⁻	SO ₄ ⁻²	Fe ⁺⁺	Mn ⁺⁺	
Concentration (mg/l)	2000	Minimum	6.1	109	6.2	3	5.6	4	27	17.9	4	1.2	0.0
		Maximum	8.1	374	26	19	46	17	68	132	26	10	0.33
		Mean	6.9	139	12.1	7.3	14	9.2	40.4	37.6	14.6	5.3	0.08
	2010	Minimum	5.9	120	10	3.8	9	3	33	21	19	0.46	0.0
		Maximum	7.5	155	21	10	14.4	13	58	44	25.3	11.8	0.2
		Mean	6.5	134	13.9	6.9	11.9	8.5	42.2	30.0	22.3	5.5	0.15
	2022	Minimum	6.4	100	9.3	4.2	9	2.9	26.5	23	15	2.2	0.16
		Maximum	7.6	370	31.9	20.8	39.8	15	60.8	131	50	7.4	0.33
		Mean	6.7	138	12.1	7.3	13.5	8.2	40.2	34.6	20.2	4.7	0.25

4. Results and Discussion

4.1. Groundwater Quality Indices Trends

4.1.1. Interpolation Method

Groundwater quality assessment in the present work involves the calculation and evaluation of five quality indices, namely TDS, EC, SAR, SO₄²⁻ and HCO₃⁻ over 22 years in three periods (2000, 2010, and 2022). Using the optimal interpolation model selection

shown in Figure 6a–e, and depending upon the least root-mean-square error, ordinary Kriging, IDW, and RBF were employed to assess groundwater quality. Generally, water containing dissolved solids greater than 1000 mg L^{-1} has an unpleasant flavor or is unfit for consumption [60]. Thus, in the research site, the levels of TDS varied from 109 to 374 mg L^{-1} in 2000, 120 to 155 mg L^{-1} in 2010, and 100 to 370 mg L^{-1} in 2022. Higher TDS values can be observed to decrease in both periods, 2000 and 2010, while in 2022, the TDS values increased in some spots in the southwest of the research region as a result of the increase in withdrawal rates in that area for agricultural activities (Figure 6a). It can be seen from Figure 6b that the amount of EC in 2000 was lower in the north and higher southeast of the research region (more than 584). Because of the land-use alterations and the reduction in precipitation, the EC values rose in some locations southwest of the research area in 2022. In contrast, the levels of SAR ranged from 0.55 to 1.67 in 2000, 0.50 to 0.80 in 2010, and from 0.50 to 1.40 in 2022. The spatial distribution map of SAR showed a significant increase in SAR values from 2000 to 2010 and in some spots in the southwest of the research region in 2022 (Figure 6c). SO_4^{2-} values varied greatly between 2000 and 2022, as shown in Figure 6d. In 2000, this parameter ranged from 27 meq L^{-1} on the north and south side to more than 68 meq L^{-1} in the area on the east and west sides of the Oasis. From 2000 to 2010, there was a considerable decline in HCO_3^- , where the concentration dropped from 68 to 58 meq L^{-1} , while the HCO_3^- values increased in some areas north and west of the study area to reach 60.8 meq L^{-1} in 2022 (Figure 6e). Both SO_4^{2-} and HCO_3^- values exhibited significant increase trends from 2000 to 2010. The increasing trends of the SO_4^{2-} and HCO_3^- values matched with the distribution map, which was slightly low over all the study sites in 2000 and then extremely high in most parts of the area between 2010 and 2022.

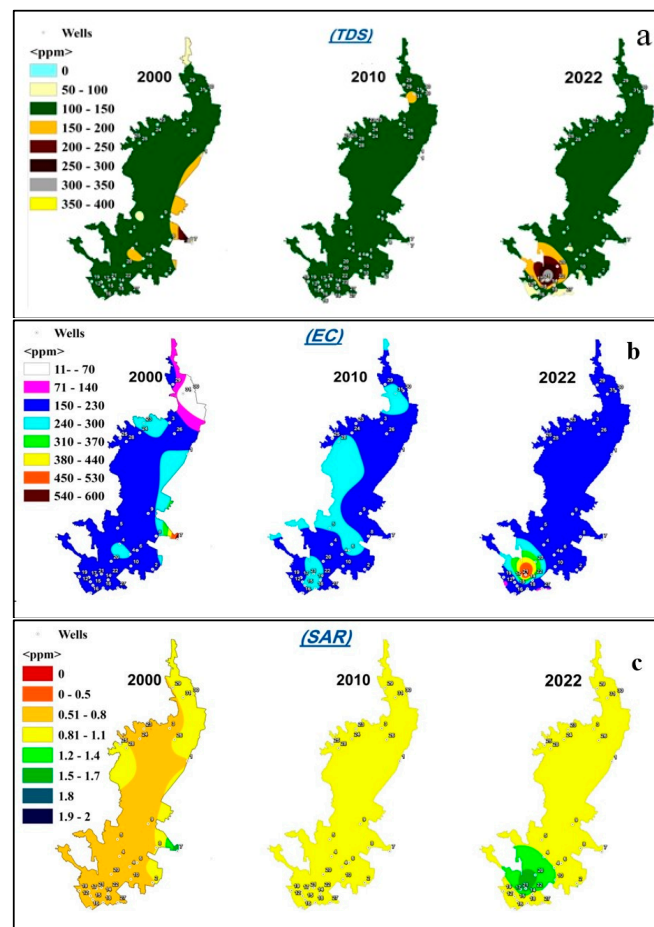


Figure 6. Cont.

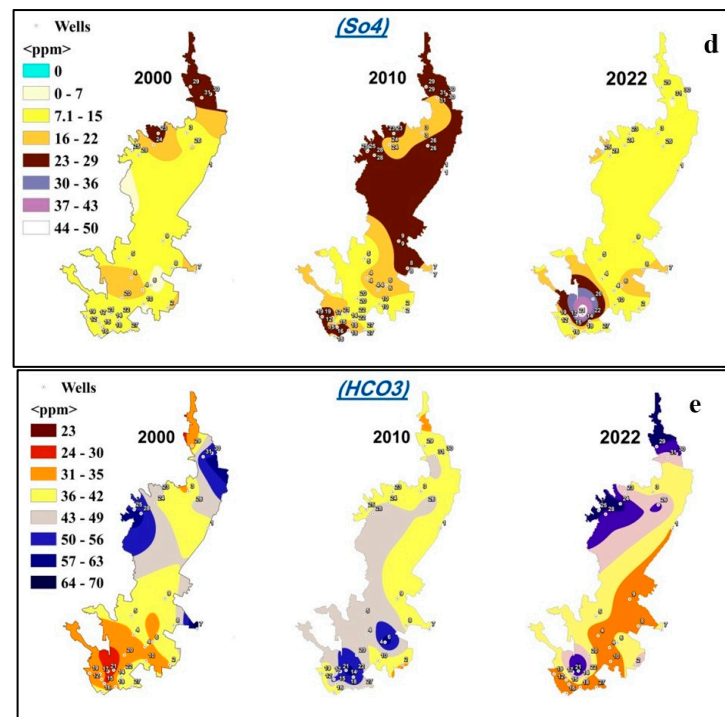
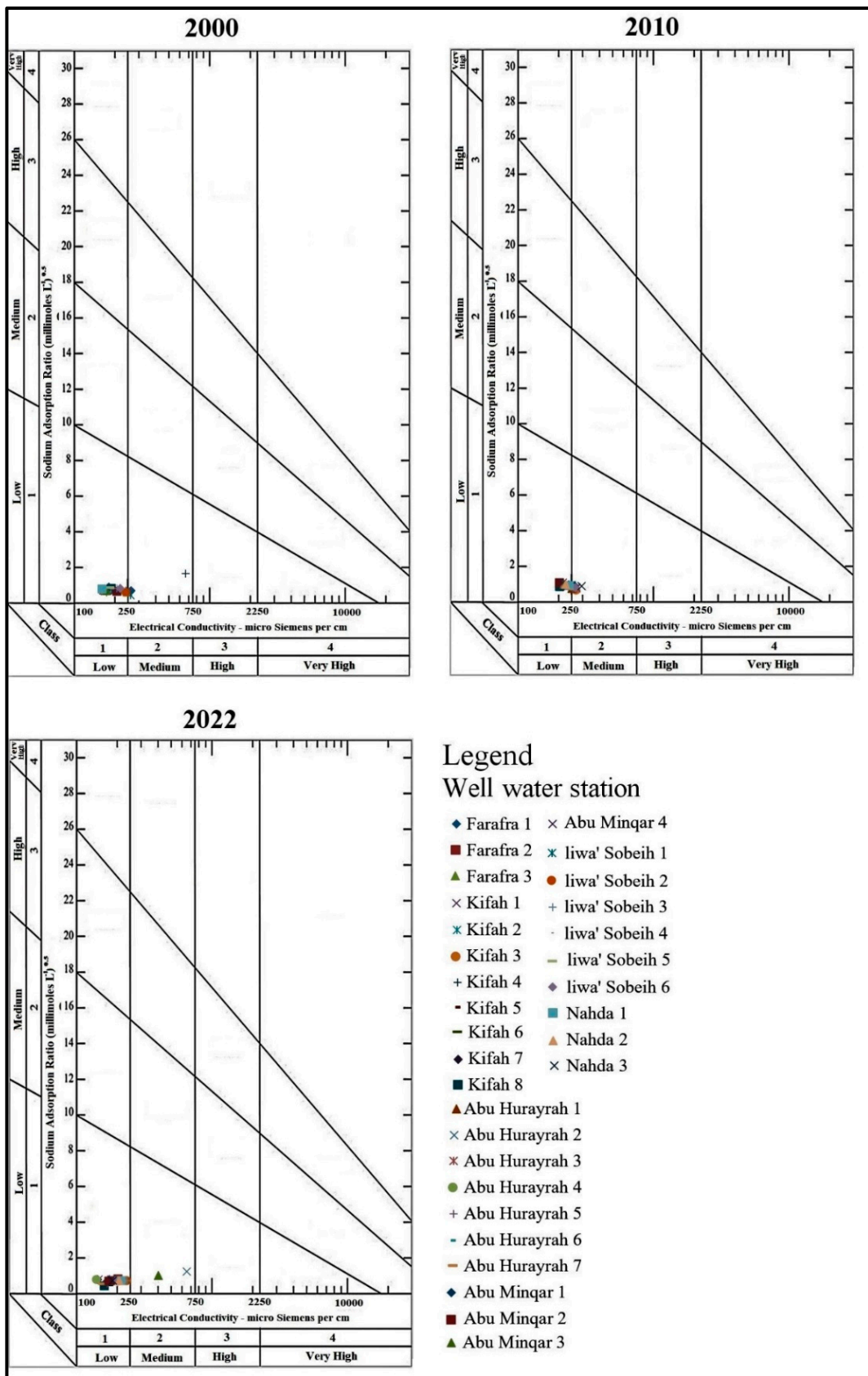


Figure 6. Spatial variations of (a) TDS, (b) EC, (c) SAR, (d) SO_4^{2-} , and (e) HCO_3^- in 2000, 2010, and 2022.

4.1.2. Schoeller and Wilcox Diagrams

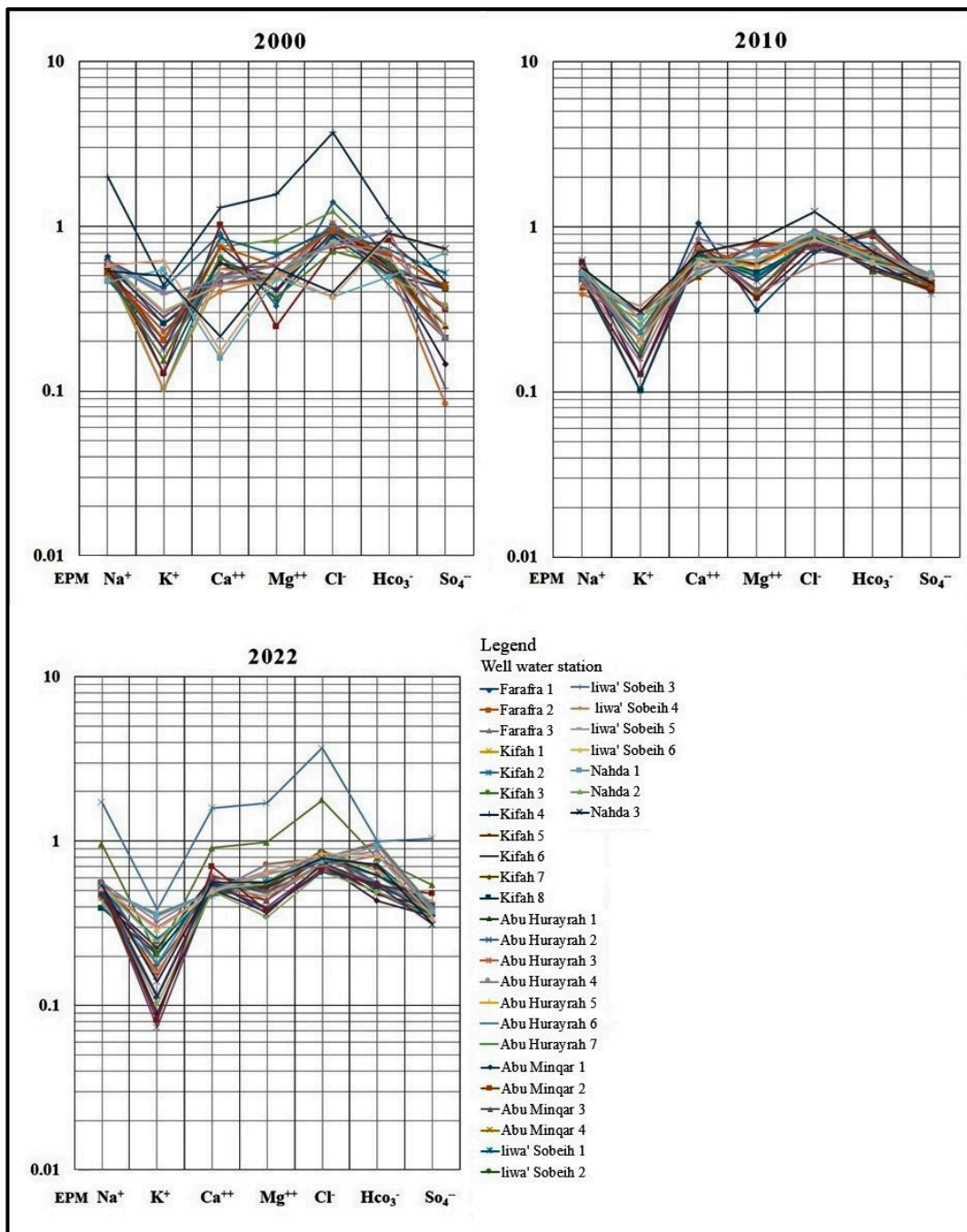
Based on the water's ionic compositions and total soluble salts, Wilcox and Schoeller's diagrams have been employed to assess the quality of water for agricultural and drinking purposes. In the Wilcox diagram [57], two parameters were determined using the Aq. Qa software (EC and SAR). In this method, salinity hazard is used to categorize water quality into S1, S2, S3, and S4 types, and sodium hazard into C1, C2, C3, and C4 types. The significance of quality ratings is described as follows: extremely good (C1S1), good (C1S2, C2S2, and C2S1), medium or acceptable (C3S3, C3S2, C3S1, C2S3, and C1S3), and poor (C4 or S4). The Schoeller diagram is a semi-logarithmic graph of the major ion concentrations in milliequivalents per liter that depicts many hydrochemical water sorts that share the same feature [58]. It is based on five chemical factors: hardness, total dissolved solids (TDS), sodium, chloride, and sulfate. By using this diagram, water is divided into six categories: good, acceptable, medium, poor, very poor, and unfit for anthropological usage.

The hydrochemical data were shown in standard graphs to compare the chemical characteristics of the region's groundwater with the World Health Organization's (WHO) standard recommendation for drinking and irrigation purposes [61]. Figure 7a,b depict the graphs created by Schoeller and Wilcox for 31 groundwater samples for the required time periods (2000, 2010, and 2022). The Schoeller graphic shows that the groundwater quality at the prescribed period was drinkable. The Wilcox graphic showed that most wells' groundwater quality has been good (C1S1) and (C2S1) for three years. Results of groundwater changes related to agriculture (Wilcox diagram) and drinking (Schoeller diagram) indicated that variations in the quality class of water were minimal and suitable for drinking and irrigation.



(a)

Figure 7. Cont.



(b)

Figure 7. (a) Groundwater quality evaluation according (Wilcox diagrams, [57]). (b) Schoeller semi-logarithmic nomogram for the groundwater samples representation in the study area.

4.1.3. Groundwater Quality Index (GWQI)

The water quality index (WQI) method is used to assess the quality of surface and groundwater for drinking [62]. In this method, the weights of several quality characteristics are likely inversely correlated to their respective variables [63]. The weight factor (between 1 and 5) is then assigned to each of the ten parameters, including pH, TDS, EC, TH, Cl^- , HCO_3^- , SO_4^{2-} , Mg^{2+} , Ca^{2+} , and Na^+ , according to their impact on groundwater quality and health. Some equations are used to determine the GWQI index (Equations (1)–(3)), depicts the findings of this method. This method results in three classes of groundwater quality excellent, good, and bad for drinking in the presence of high concentrations of

iron and manganese. Without iron and manganese concentrations, the excellent class of groundwater quality for drinking in all groundwater samples.

$$W_{ri} = wi / \sum_{i=1}^n wi \quad (1)$$

where (w_i) and (W_{ri}) are, respectively, the weight and relative weight of each chemical parameter. Qualitative rank for each of them (q_i) calculated using Equation (2)

$$(q_i) = \frac{C_i}{S_i} \times 100 \quad (2)$$

where (C_i) is the concentration of each chemical parameter and (S_i) is WHO standard values. Finally, the GWQI index is calculated according to Equation (3).

$$GWQI = \sum_{i=1}^n (W_{ri} \times q_i) \quad (3)$$

Furthermore, land use change was mapped during the specified period of time to identify the areas where groundwater quality has changed as a consequence of land use modification using change detection and supervised classification methods by GIS techniques (ArcMap 10.5) [64]. Three Landsat satellite images (2000, 2010, and 2022) (Figure 8a–c) encompassing the research region were used by the American Geological Survey (https://pubs.usgs.gov/gip/gw_ruralhomeowner/) (accessed on 1 January 2023) after radiometric and atmospheric correction to them using ENVI 5.3 [65] software. Climatic condition data for the specific (2000–2022) were mainly acquired from the site ([Earthexplorer.usgs.gov](https://earthexplorer.usgs.gov)). While the Demographic data was collected from the official reports of the central agency for public mobilization & Statistics (CAPMAS).

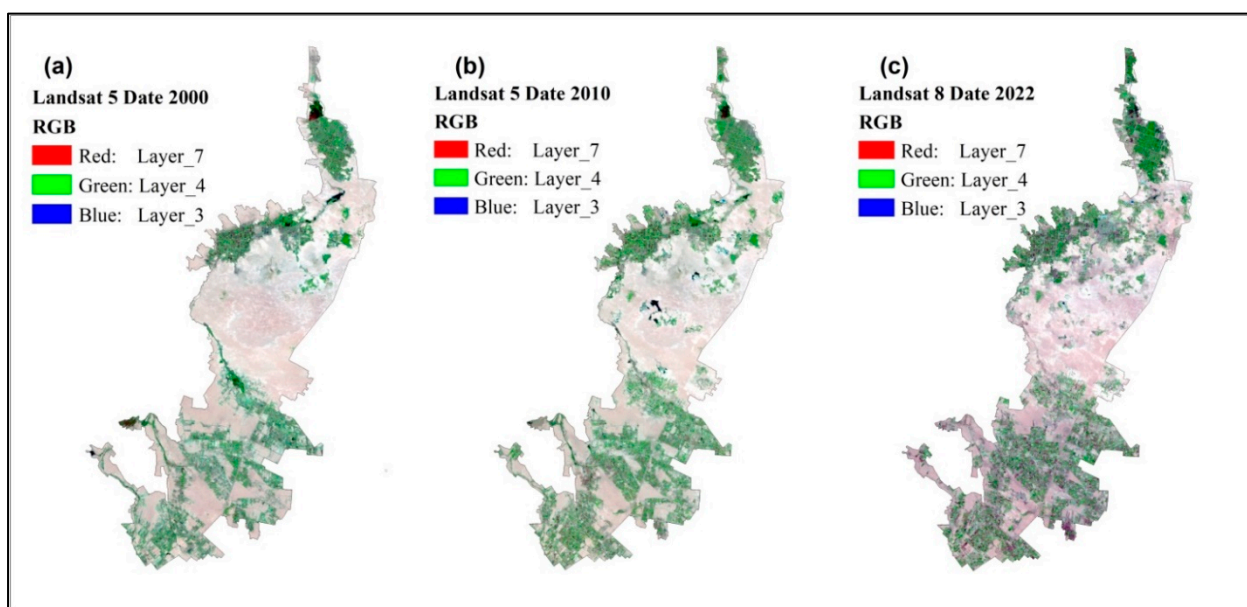


Figure 8. Landsat satellite image characteristics within the research region; (a) Landsat 5 from 2000, (b) Landsat 5 from 2010, and (c) Landsat 8 from 2022.

The chemical analyses from 2000, 2010, and 2022 were used to calculate the GWQI index, which was employed to evaluate changes in groundwater quality for consumption. In 2000, the GWQI index showed a significant decrease. While in 2010, the index shows that the quality of water in the research region has been high. However, in this period, changes were unregular. In 2010, water quality increased compared to 2022. In the research region,

the concentration of iron in the groundwater samples ranged from 1.16 to 10 mg L⁻¹ (2000), 2.28 to 11.80 mg L⁻¹ (2010), and 2.2 to 7.42 mg L⁻¹ (2022). Additionally, the concentration of manganese ranged from 0.01 to 0.3 mg L⁻¹ (2000), 0.00 to 0.20 mg L⁻¹ (2010), and 0.17 to 0.33 mg L⁻¹ (2022). In the presence of extremely high concentrations of iron and manganese as a consequence of soil degradation and the development of residential areas, the index has grown in all wells, indicating that the groundwater quality has worsened in almost all wells (Figure 9a,b).

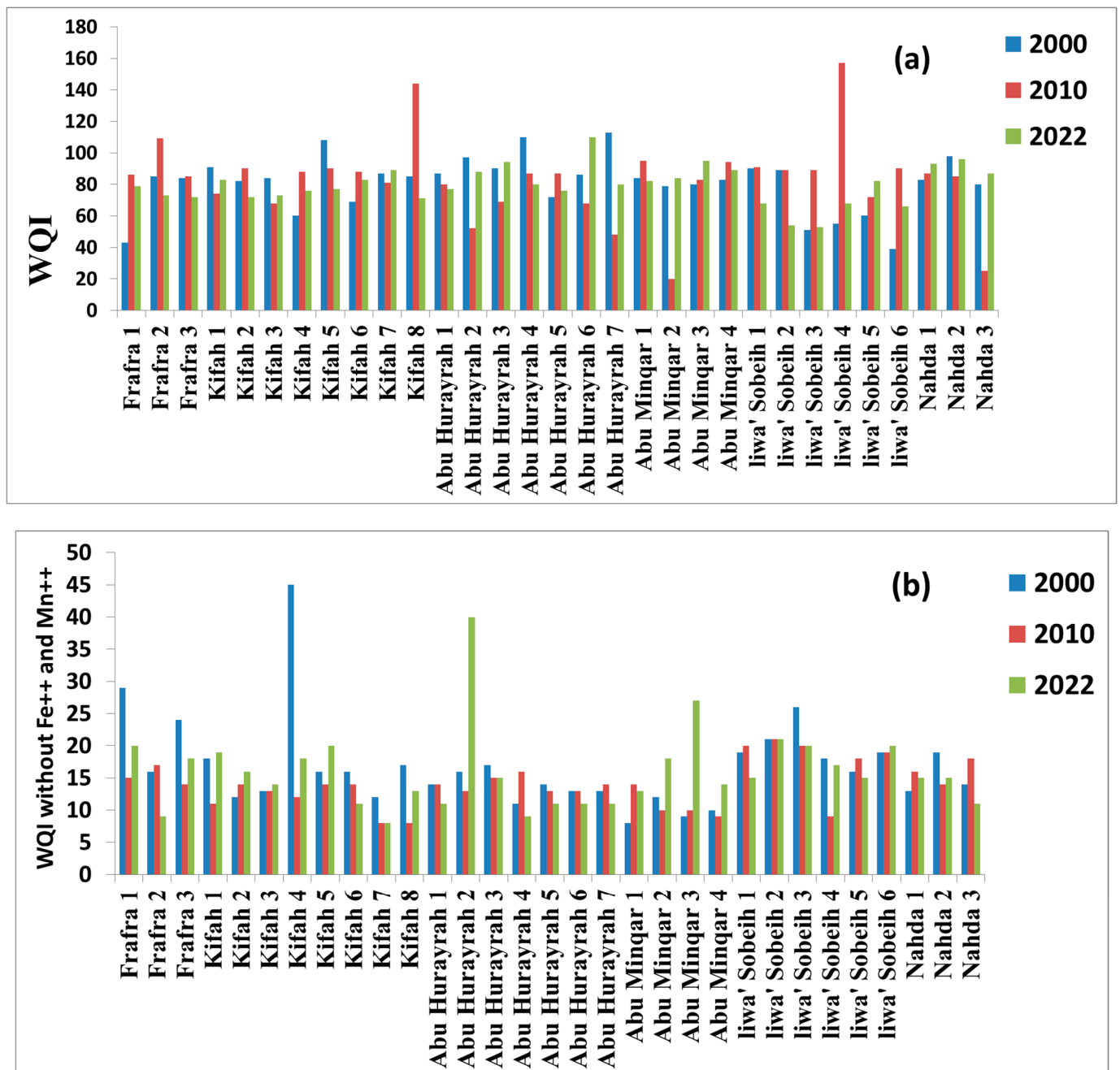


Figure 9. GWQI index; (a) with and (b) without Fe²⁺ and Mn²⁺ concentration in 2000, 2010, and 2022.

4.2. Impacts of Altering Land Use on the Quality of Groundwater

Various researchers [66–68] have investigated the impact of an extensive expansion of agriculture and other parameters on groundwater and soil quality. Alterations in land use are strongly implicated as one of the most important human-caused variables affecting

the soil and underground water system [69]. Although the footprint of the land used and climate changes on water quality degradation, this linkage has not been widely explored in Egypt; however, this linkage has long been recognized globally. Tang et al. [70] and Bhaduri et al. [71] concluded that land-use alterations significantly affect the watershed region’s hydrology. In the latest two decades, the geographical distribution patterns of alterations in land use in the studied region revealed an expansion of agricultural fields.

The Oasis is 160.18 km² in total area. Four types of land usage were distinguished, urban, water, agricultural, and barren lands (Figure 10). Among the types of land use changes in the area is extending the agriculture area from 2000 to 2022 using flooded water for irrigation. This greatly influenced the quality of groundwater because of the too much water extraction in the region. Under arid conditions which characterized the study area, similarly, land use changes influenced aquifer recharge rates. The categorization of satellite images revealed that the proportion of agricultural land in the study region changed from 12.8% in 2000 to 13.3% in 2010 to 14.6% in 2022. Figure 11 depicts the changes in land use, while Table 2 provides a percentage comparison of these alterations. The change in percentage of the urban area was 6.4% in 2000, 7.8% in 2010, and it increased to 11.1% in 2022. As represented in the study area by springs, the water category was less than 1% in 2000, 0.3% in 2010, and decreased to 0.2% in 2022. The spreading out of farming land contributes to worsening groundwater quality; this deterioration is ascribed to the increased use of chemical fertilizers in the studied region. Alternatively, pollution and change in discharge may be a consequence of land use variations related to rigorous farming activities. Throughout the analysis of land use changes percentage through the study periods, especially the agricultural practice and anthropogenic activities may increase the degrading of groundwater quality in the area.

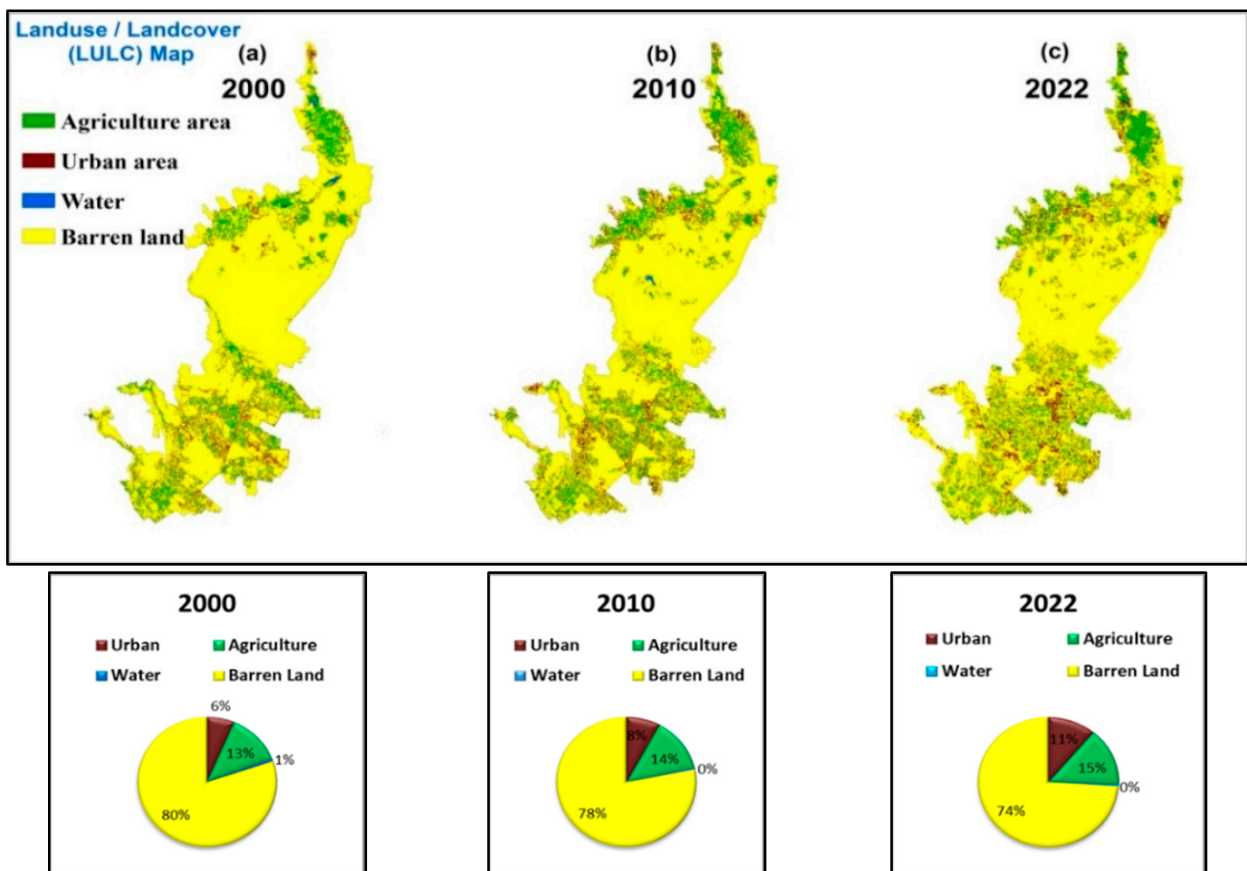


Figure 10. Land use/land cover map and percentage of the study area in (a) 2000, (b) 2010, and (c) 2022.

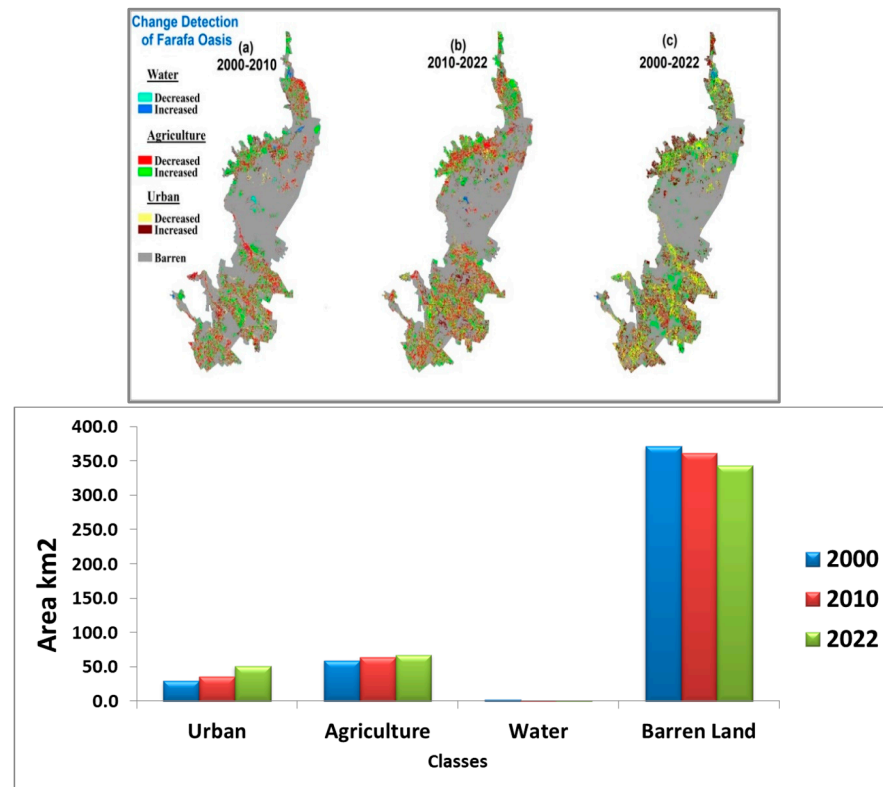


Figure 11. Change detection of land use in El-Farafra Oasis over the study periods. (a) represents changes between 2000 and 2010. (b) represents changes between 2010 and 2022. (c) represents changes between 2000 and 2022.

Table 2. Summary of the land use areas and percentage over the study periods.

Years	Agriculture	Urban	Water	Barren lands	Total
2000	59.4 (12.8%)	29.6 (6.4%)	2.9 (0.6%)	371.7 (80.2%)	463.6 (100%)
2010	63.9 (13.8%)	36.3 (7.8%)	1.4 (0.3%)	362.0 (78.1%)	463.6 (100%)
2022	67.8 (14.6%)	51.3 (11.1%)	1.3 (0.2%)	343.2 (74.0%)	463.6 (100%)

4.3. Impacts of Climate Change on Groundwater Quality

Due to the lack of climatic stations on the study site, detailed knowledge of the climate condition in the study area was obtained from the power access data viewer web (<https://power.larc.nasa.gov>) (accessed on 1 January 2023). The acquired information includes maximum atmospheric temperature and means annual rainfall. The annual climate indicators (maximum temperature and mean precipitation) during 2000, 2010, and 2022 are shown in Figure 12. The highest average temperature was 39 °C and was recorded in July, while the lowest average through the last 22 years was recorded in January and was 10 °C. The highest mean relative humidity in the study area was 60%, recorded in December, and the lowest was 33% in May. In 2020, the maximum annual average precipitation in this area was 6.15 mm. The variation in precipitation indicates that the quantity of precipitation fell from 2000 to 2022 but was at its minimum in 2000, 2009, 2012 to 2015, and 2019, indicating dryness in such periods. However, the climate conditions in the area indicate a slight overall increase in the atmospheric temperature (Figure 12a), with an increase in annual rainfall during the years 2011, 2016, and 2020 (Figure 12b).

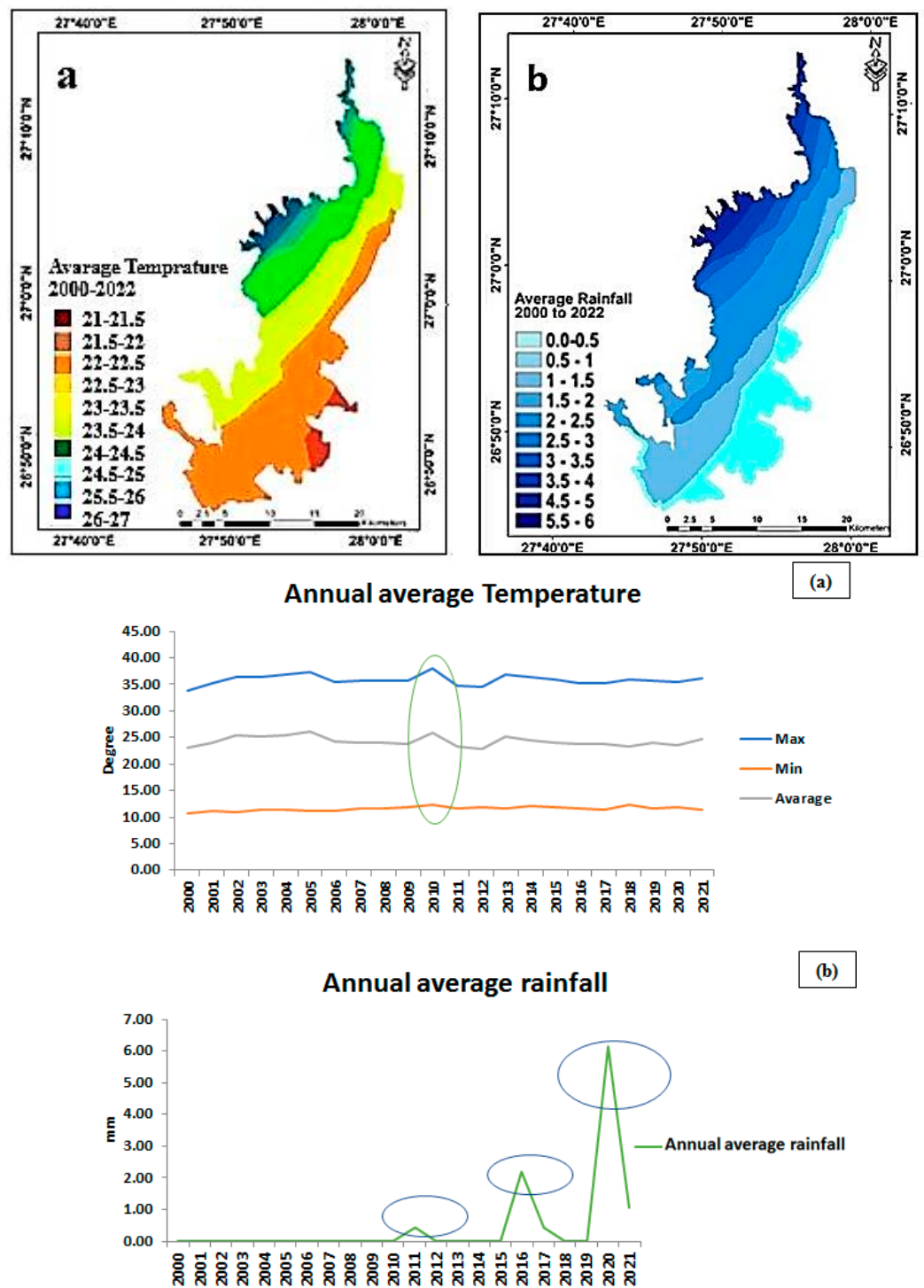


Figure 12. Climatological data of El-Farfra Oasis, Annual averages during the period (2000–2022) (average of latest 22 years) (<https://power.larc.nasa.gov>) (accessed on 1 January 2023). (a) annual average temperature. (b) annual average rainfall.

In 2009, the maximum atmospheric temperatures exhibited higher temperatures. On the other hand, comparing the annual maximum temperatures in the years 2000, 2010, and 2022, the results indicated that the approximate temperatures are 23.10, 25.35, and 24.72 °C, respectively. Furthermore, the increasing temperature will lead to an increased evaporation process, thus impacting the groundwater systems with a depth to the water table of 10 m or less. However, the precipitation trend during the study period showed slight changes and increases in the precipitation rates in 2010, 2016, and 2010. An increase in annual

precipitation is associated with an increase in the frequency of extreme precipitation events causing flash floods. The increasing precipitation in the area could lead to an increase in the aquifer recharge through surface runoff. These climatic conditions, linked with a geological context, may have led to the decreased water residence time in the aquifer, allowing water movement and degrading the water quality with greater water-rock interaction.

Finally, land use and climate change significantly affected groundwater quality degradation in the area. In particular, the increase in extreme and irregular climatic events such as rainfall and temperature have an impact on water quality. The higher temperatures in all cases are linked to higher evapotranspiration, which is most severe during summer. By comparing the precipitation during the study periods, no major change was observed in the rainfall rate except in the years 2010, 2016, and 2020. The annual precipitation in 2010 was 0.44 mm, then declined to 0.00 mm until it increased again to 2.20 mm in 2016 and 6.15 mm in 2020. From the perspective of geology combined with structural conditions, several investigations have underlined groundwater quality alterations induced by the seepage from different aquifers along with the fault system.

4.4. Population Growth Impacts on Groundwater Quality

The observed changes in population growth are closely related to the depletion of groundwater level and quality in the study area. El-Farafra Oasis in Egypt has experienced significant population growth, with an annual rate of 7.52% between 2000 and 2020 with a total population 35,820 per based on The Central Agency for Public Mobilization and Statistics (CAPMAS) reports (Figure 13). Farafra has a relatively high population density ranging from 207 to 1573 individuals per square kilometer (Figure 14). However, this growth has put pressure on the limited natural resources in the area, particularly the groundwater supplies which are decreasing at a rate of $284.34 \times 10^6 \text{ m}^3/\text{year}$. Maintaining water quality is crucial for the well-being of society, especially with the increasing demand for water, energy, land, and infrastructure due to urbanization. Neglecting the issue of water pollution could result in a future where polluted water is the only option for drinking.

El-Farafra Oasis heavily relies on groundwater for drinking water due to its distance from the Nile River, making it critical to maintain its quality during population growth. However, population growth has created a disproportion between the availability of fresh water and the number of people relying on it, resulting in pressure on groundwater quality. The effects of this pressure are complex and depend on a range of factors, including scientific, social, economic, and management factors.

4.5. Water Quality Spatial Model

The research employed several water quality spatial models (WQSM) using ArcGIS software (V.10.8) to identify the most areas where the groundwater quality is most affected based on the main implemented factors. The models' input included main variables, i.e., chemical analysis, land uses, population growth and climatic data. The results of each model are classified into five classes including; high-risk, moderately high, moderate, moderately low, and low-risk areas (Figure 15). Accordingly, chemical analysis and land use had the highest importance values in the modeling process. On the other hand, climate change and Population growth had the least important values. Inspection of the final model output (Figure 16) indicates that, the area where the groundwater quality is the most affected lies in the north of the Oasis (Alamil Oasis) which is an area where agricultural areas are increasing, elements concentrations and population density. While the central region of the Oasis is found to be the least affected (Al shaykh Marzuq and Al shaykh Marzuq Aljadida area) where agricultural areas and populations decrease significantly from models for different indices (Figure 16).

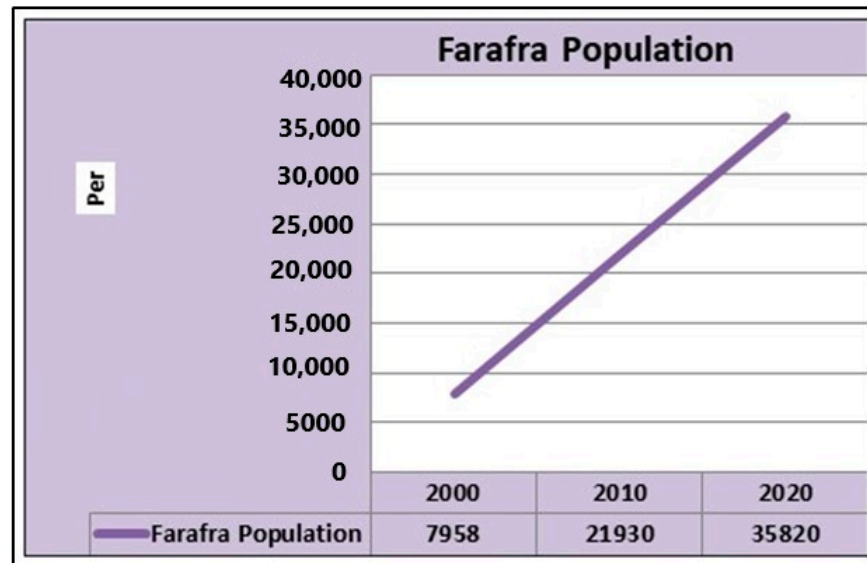


Figure 13. Population growth of El-Farafra Oasis from 2000 to 2020.

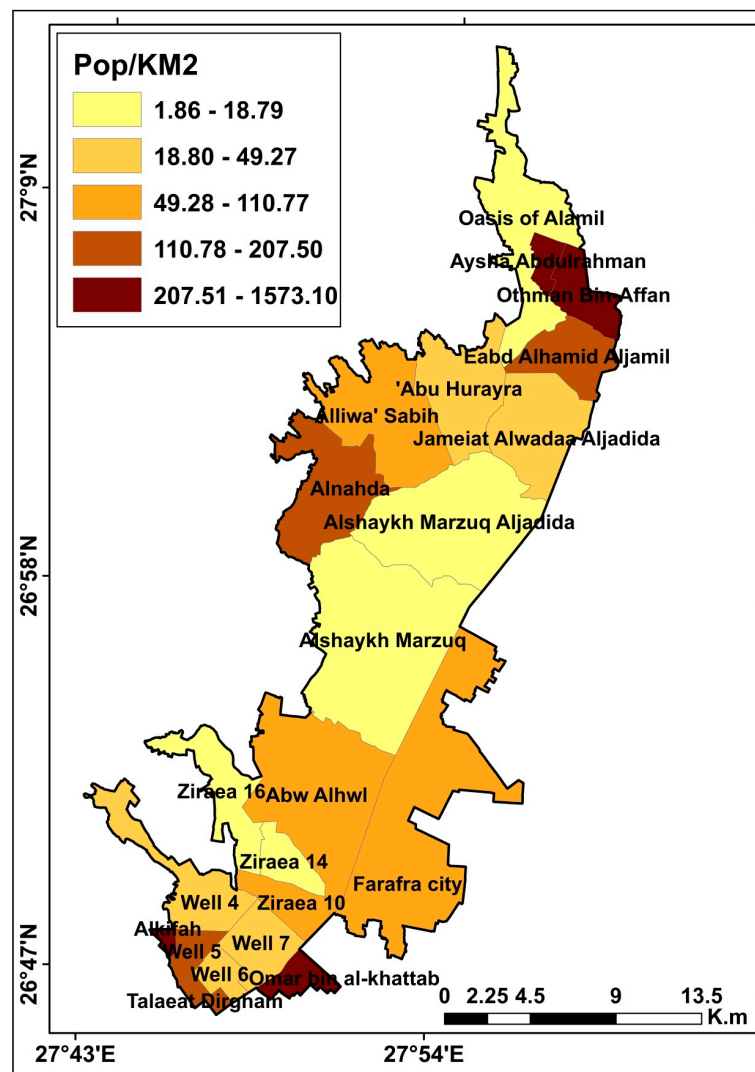


Figure 14. Geographical distribution of the population density of Farafra Oasis in 2020.

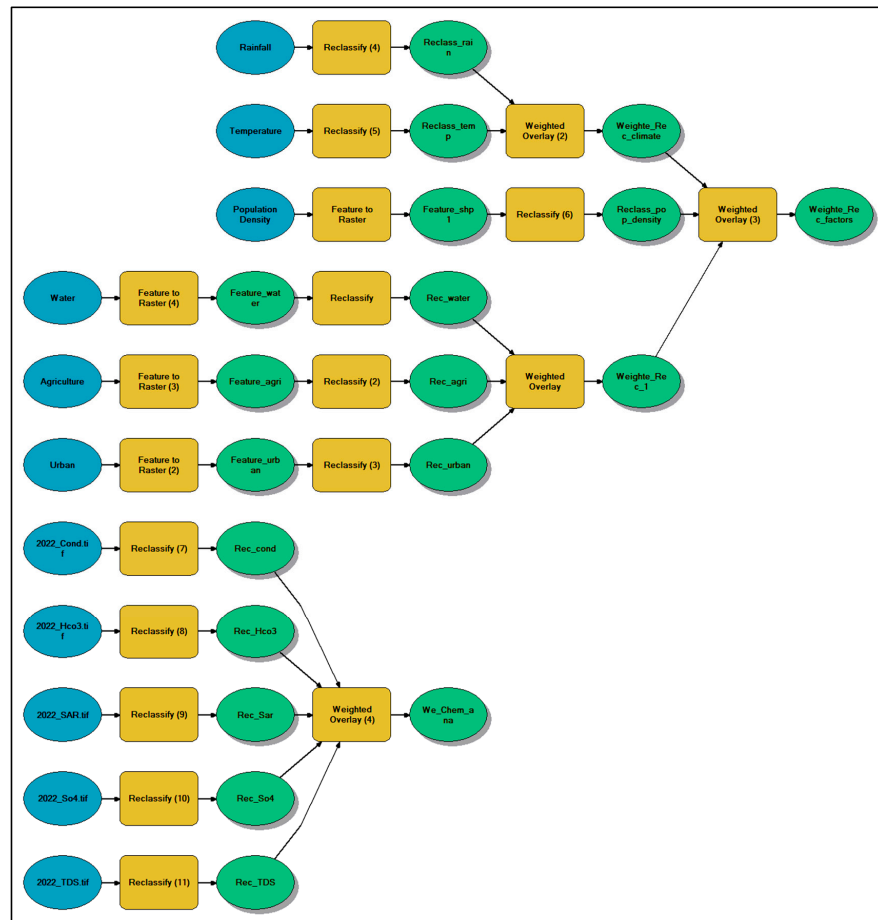


Figure 15. Flow chart of Water resources potentiality model.

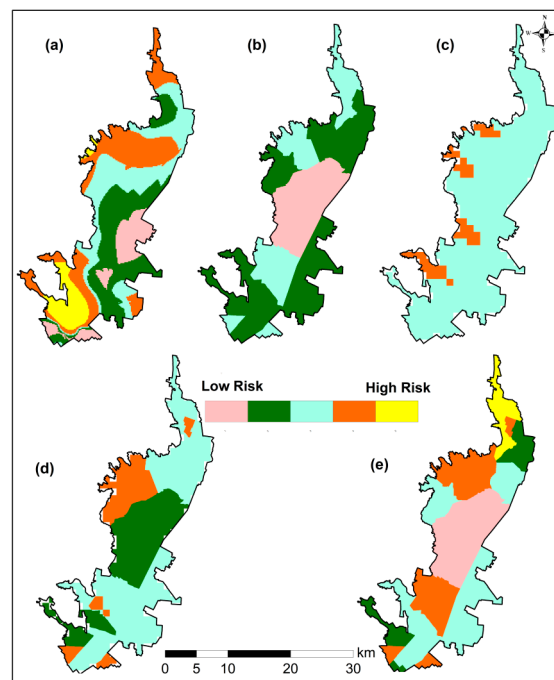


Figure 16. Spatial model of each indices (a) Chemical analysis, (b) Landuse, (c) Climate change, (d) Population growth, and (e) The final model.

The groundwater content in Nubia sandstone are free of nitrates based on the studied stated that only deep percolation only reach the surface wells and no pollutant seeps into the deep wells in the area according to Metwaly et al. [72].

5. Conclusions

The findings revealed differences in groundwater quality indices (TDS, SAR, SO_4^{-2} and HCO_3^-) over time. A significant increase was observed in these indices from 2000 to 2022. According to the distribution maps, the majority of groundwater quality indices in the region are projected to be very high in 2022 (370 mg L^{-1} , 0.5–1.4, 27 mg L^{-1} , and 60.8 mg L^{-1} , respectively), according to the distribution maps. The results show an increase in the population growth and urban areas in the Oasis between 2000 and 2022 (7.52% per year and 51.3 km^2 , respectively). No major change was observed in the rainfall rate except in the years 2010, 2016, and 2020 (0.44 mm, 2.20 mm, and 6.15 mm). Thus, the effect of climatic changes on the groundwater quality in the study area is negligible. Hence, this will increase the demand for groundwater, so deterioration and future unsustainability will be existing. Consequently, it may be noted that groundwater quality decline typically happens. Land use changes revealed an increase in the agriculture area between 2000 to 2022 (from 12.8% in 2000 to 14.6% in 2022). Land use changes revealed an increase in the agriculture area between 2000 to 2020. The use of nitrogen-based synthetic fertilizers and flooding irrigation in agriculture, as well as high concentrations of iron and manganese, may alter and impair the quality of groundwater in the region. Consequently, the modifications in groundwater quality may result from intense agricultural practices, climate change, or other human activities in the area. Many ways are used to treat the presence of Fe^{2+} and Mn^{2+} in groundwater, the installation of a water softener is meant to remove them if they are present at minute levels, and the filtering procedure utilized precipitates iron from water in which oxygen is added. Other treatments, such as chlorination, feeding ozone or hydrogen peroxide, and removal by potassium permanganate feed with manganese green sand filters, and some newly developed synthetic media, might be used. According to the final output of the suggested model, groundwater quality is high in large extended areas of the central part of the Oasis (about 108.22 km^2), while, low groundwater quality was detected in the northern part of the investigated Oasis, occupying a small area (31.8 km^2). The low water quality in these northern parts of the study area is attributed to the impacts of climate changes, population growth, and land-use factor. Overall, the presented model is essential for tackling future challenges faced by arid and semiarid regions.

Author Contributions: Conceptualization, H.A.M., H.M.G., R.H.R., M.A.E.A., P.D., A.S. and M.H.D.; methodology, H.A.M., H.M.G., R.H.R., M.A.E.A., P.D., A.S. and M.H.D.; software, H.A.M., H.M.G., R.H.R., M.A.E.A. and M.H.D.; validation, H.A.M., M.A.E.A., P.D., A.S. and M.H.D.; formal analysis, H.A.M., M.A.E.A. and M.H.D.; investigation, H.A.M., M.A.E.A. and M.H.D.; resources, H.A.M., M.A.E.A. and M.H.D.; data curation, H.A.M., M.A.E.A. and M.H.D.; writing—original draft preparation, H.A.M., M.A.E.A., P.D., A.S. and M.H.D.; writing—review & editing, H.A.M., M.A.E.A., P.D., A.S. and M.H.D.; visualization, H.A.M., M.A.E.A. and M.H.D.; supervision, H.A.M., M.A.E.A. and M.H.D.; project administration, H.A.M., M.A.E.A., A.S. and M.H.D.; funding acquisition, H.A.M., M.A.E.A., P.D., A.S. and M.H.D. All authors have read and agreed to the published version of the manuscript.

Funding: This research received no external funding.

Institutional Review Board Statement: Not applicable.

Data Availability Statement: Not applicable.

Acknowledgments: The manuscript presents a participation between the scientific institutions in two countries (Egypt and Italy), and in particular, the authors are grateful for their support in carrying out the work to: (1) National Authority for Remote Sensing and Space Sciences (NARSS), Cairo 11769, (2) Geology Department, Faculty of Science, New Valley University, El Kharga 72511, Egypt. (3) SAFE-Università degli Studi della Basilicata—Potenza, (4) Ministero dello Sviluppo Economico

(La casa delle tecnologie; il giardino delle tecnologie emergenti—Matera), (5) PSR 16.2 ‘Smart Irrifert’ project CUP: G19J21004870006, (6) MIUR- PNRR-Tech4you.

Conflicts of Interest: The authors would like to hereby certify that no conflict of interest in the data collection, analyses, and the interpretation; in the writing of the manuscript, and in the decision to publish the results. Authors would like also to declare that the funding of the study has been supported by the authors’ institutions.

References

- Riedel, T.; Kübeck, C. Uranium in groundwater—A synopsis based on a large hydrogeochemical data set. *Water Res.* **2018**, *129*, 29–38. [[CrossRef](#)]
- Nistor, M.-M. Climate change effect on groundwater resources in South East Europe during 21st century. *Quat. Int.* **2019**, *504*, 171–180. [[CrossRef](#)]
- Rajaei, F.; Dahmardeh Behrooz, R.; Ahmadisharaf, E.; Galalizadeh, S.; Dudic, B.; Spalevic, V.; Novicevic, R. Application of integrated watershed management measures to minimize the land use change impacts. *Water* **2021**, *13*, 2039. [[CrossRef](#)]
- El-Magd, S.A.A.; Ahmed, H.; Pham, Q.B.; Linh, N.T.T.; Anh, D.T.; Elkhachy, I.; Masoud, A.M. Possible factors driving groundwater quality and its vulnerability to land use, floods, and droughts using hydrochemical analysis and GIS approaches. *Water* **2022**, *14*, 4073. [[CrossRef](#)]
- Cuthbert, M.O.; Gleeson, T.; Moosdorf, N.; Befus, K.M.; Schneider, A.; Hartmann, J.; Lehner, B. Global patterns and dynamics of climate-groundwater interactions. *Nat. Clim. Chang.* **2019**, *9*, 137–141. [[CrossRef](#)]
- Bounoua, L.; Nigro, J.; Zhang, P.; Thome, K.; Lachir, A. Mapping urbanization in the United States from 2001 to 2011. *Appl. Geogr.* **2018**, *90*, 123–133. [[CrossRef](#)]
- Woodrow, K.; Lindsay, J.B.; Berg, A.A. Evaluating DEM conditioning techniques, elevation source data, and grid resolution for field-scale hydrological parameter extraction. *J. Hydrol.* **2016**, *540*, 1022–1029. [[CrossRef](#)]
- Xiao, Y.; Liu, K.; Zhang, Y.; Yang, H.; Wang, S.; Qi, Z.; Hao, Q.; Wang, L.; Luo, Y.; Yin, S. Numerical investigation of groundwater flow system and its evolution under the climate change in the arid Golmud river watershed on Tibetan Plateau. *Front. Earth Sci.* **2022**, *10*, 943075. [[CrossRef](#)]
- Darwish, M.H.; Galal, W.F. Spatiotemporal effects of wastewater ponds from a geoenvironmental perspective in the Kharga region, Egypt. *J. Prog. Phys. Geogr. Earth Environ.* **2020**, *44*, 376–397. [[CrossRef](#)]
- Darwish, M.H.; Megahed, H.A.; Farrag, A.A.; Sayed, A.G. Geo-Environmental Changes and Their Impact on the Development of the Limestone Plateau, West of Assiut, Egypt. *J. Indian Soc. Remote Sens.* **2020**, *48*, 1705–1727. [[CrossRef](#)]
- Galal, W.F.; Darwish, M.H. Geoenvironmental assessment of the mut wastewater ponds in the Dakhla Oasis, Egypt. *Geocarto Int.* **2020**, *37*, 3293–3311. [[CrossRef](#)]
- Xiao, Y.; Hao, Q.; Zhang, Y.; Zhu, Y.; Yin, S.; Qin, L.; Li, X. Investigating sources, driving forces and potential health risks of nitrate and fluoride in groundwater of a typical alluvial fan plain. *Sci. Total Environ.* **2022**, *802*, 149909. [[CrossRef](#)]
- Xiao, Y.; Liu, K.; Hao, Q.; Xiao, D.; Zhu, Y.; Yin, S.; Zhang, Y. Hydrogeochemical insights into the signatures, genesis and sustainable perspective of nitrate enriched groundwater in the piedmont of Hutuo watershed, China. *Catena* **2022**, *212*, 106020. [[CrossRef](#)]
- Rehana, S.; Mujumdar, P.P. River water quality response under hypothetical climate change scenarios in Tunga-Bhadra river, India. *Hydrol. Process.* **2011**, *25*, 63373–63386. [[CrossRef](#)]
- Hu, Z.; Wang, L.; Wang, Z.; Hong, Y.; Zheng, H. Quantitative assessment of climate and human impacts on surface water resources in a typical semi-arid watershed in the middle reaches of the Yellow River from 1985 to 2006. *Int. J. Climatol.* **2015**, *35*, 97–113. [[CrossRef](#)]
- Sang, Y.-F.; Wang, Z.; Liu, C.; Yu, J. The impact of changing environments on the runoff regimes of the arid Heihe River basin, China. *Theor. Appl. Climatol.* **2014**, *115*, 187–195. [[CrossRef](#)]
- Hasan, S.S.; Zhen, L.; Miah, M.-G.; Ahamed, T.; Samie, A. Impact of land use change on ecosystem services: A review. *Environ. Dev.* **2020**, *34*, 100527. [[CrossRef](#)]
- Velazquez, M.P.; Haro, S.P.; Garcia-Prats, A.; Mocholi-Almudever, A.F.; Henriquez, L. Integrated assessment of the impact of climate and land use changes on groundwater quantity and quality in the Mancha Oriental system (Spain). *Hydrol. Earth Syst. Sci.* **2015**, *19*, 1677–1693. [[CrossRef](#)]
- Fu, B.; Qiu, Y.; Wang, J.; Chen, L. Effect simulations of land use change on the runoff and erosion for a gully catchment of the Loess Plateau, China. *Acta Geogr. Sin.* **2002**, *57*, 717–722.
- Zhang, L.; Dawes, W.R.; Walker, G.R. Response of mean annual evapotranspiration to vegetation changes at catchment scale. *Water Resour. Res.* **2001**, *37*, 701–708. [[CrossRef](#)]
- Huang, M.; Zhang, L. Hydrological responses to conservation practices in a catchment of the Loess Plateau, China. *Hydrol. Process* **2004**, *18*, 1885–1898. [[CrossRef](#)]
- Hoff, H. The water challenge: Joint Water Project. *Glob. Chang. Newsl.* **2002**, *50*, 46–48.
- Bate, G.; Mkhwanazi, M.; Simonis, J. The effects of population growth on the groundwater quality of a sandy rural catchment. *Trans. R. Soc. S. Afr.* **2018**, *73*, 243–253. [[CrossRef](#)]

24. Ojeda Olivares, E.A.; Sandoval Torres, S.; Belmonte Jiménez, S.I.; Campos Enríquez, J.O.; Zignol, F.; Reygadas, Y.; Tiefenbacher, J.P. Climate change, land use/land cover change, and population growth as drivers of groundwater depletion in the Central Valleys, Oaxaca, Mexico. *Remote Sens.* **2019**, *11*, 1290. [[CrossRef](#)]
25. Elmahdy, S.; Mohamed, M.; Ali, T. Land use/land cover changes impact on groundwater level and quality in the northern part of the United Arab Emirates. *Remote Sens.* **2020**, *12*, 1715. [[CrossRef](#)]
26. Singh, C.K.; Shashtri, S.; Mukherjee, S.; Kumari, R.; Avatar, R.; Singh, A.; Singh, R.P. Application of GWQI to assess effect of land-use change on groundwater quality in lower shivaliks of Punjab: Remote sensing and GIS based approach. *Water Resour. Manag.* **2011**, *25*, 1881–1898. [[CrossRef](#)]
27. Du, C.; Cai, F.; Zidan, M.A.; Ma, W.; Lee, S.H.; Lu, W.D. Reservoir computing using dynamic memristors for temporal information processing. *Nat. Commun* **2017**, *8*, 2204. [[CrossRef](#)]
28. Hyandye, C.; Martz, L.W. A Markovian and cellular automata land use change predictive model of the Usangu Catchment. *Int. J. Remote Sens.* **2017**, *38*, 64–81. [[CrossRef](#)]
29. Karimi, H.; Jafarnezhad, J.; Khaleidi, J.; Ahmadi, P. Monitoring and prediction of land use/land cover changes using CA-Markov model: A case study of Ravansar County in Iran. *Arab. J. Geosci.* **2018**, *11*, 592. [[CrossRef](#)]
30. Kourosh Niya, A.; Huang, J.; Karimi, H.; Keshtkar, H.; Naimi, B. Use of Intensity Analysis to Characterize Land Use/Cover Change in the Biggest Island of Persian Gulf, Qeshm Island, Iran. *Sustainability* **2019**, *11*, 4396. [[CrossRef](#)]
31. Xiao, Y.; Liu, K.; Hao, Q.; Li, Y.; Xiao, D.; Zhang, Y. Occurrence, Controlling Factors and Health Hazards of Fluoride-Enriched Groundwater in the Lower Flood Plain of Yellow River, Northern China. *Expo Health* **2022**, *14*, 345–358. [[CrossRef](#)]
32. He, Z.; Wang, Z.; Suen, C.J.; Ma, X. Hydrologic sensitivity of the upper san joaquin river watershed in California to climate change scenarios. *Hydrol. Res.* **2013**, *44*, 723–736. [[CrossRef](#)]
33. Li, P.; Tian, R.; Liu, R. Solute geochemistry and multivariate analysis of water quality in the guohua phosphorite mine, Guizhou Province. China. *Expo Health* **2019**, *11*, 81–94. [[CrossRef](#)]
34. Henri, C.V.; Harter, T.; Diamantopoulos, E. Stochastic assessment of the effect of land-use change on nonpoint source-driven groundwater quality using an efficient scaling approach. *Stoch. Env. Res. Risk Assess.* **2021**, *35*, 959–970. [[CrossRef](#)]
35. Megahed, H.A.; GabAllah, H.M.; AbdelRahman, M.A.E.; D’Antonio, P.; Scopa, A.; Darwish, M.H. Geomatics-Based Modeling and Hydrochemical Analysis for Groundwater Quality Mapping in the Egyptian Western Desert: A Case Study of El-Dakhla Oasis. *Water* **2022**, *14*, 4018. [[CrossRef](#)]
36. Houben, G.; Tünnermeier, T.; Eqrar, N.; Himmelsbach, T. Hydrogeology of the Kabul Basin (Afghanistan) Part II: Groundwater Geochemistry. *Hydrogeol. J.* **2009**, *17*, 935–948. [[CrossRef](#)]
37. Ketata, M.; Hamzaoui, F.; Gueddari, M.; Bouhila, R.; Riberio, L. Hydrochemical and statistical study of groundwater in gabessouth deep aquifer (South-eastern Tunisia). *Phys. Chem. Earth* **2011**, *36*, 187–196. [[CrossRef](#)]
38. Elçi, A.; Polat, R. Assessment of the statistical significance of seasonal groundwater quality change in karstic aquifer system near Izmir-Turkey. *Environ. Monit. Assess.* **2010**, *172*, 445–462. [[CrossRef](#)]
39. Malakutian, M.; Karami, A. Chemical quality variability in groundwater of Bam plain from 1998–2004. *Clin. J. Hormozgan* **2004**, *2*, 101–109.
40. Mohammadi, M.; Ghaleney, M.M.; Ebrahimi, E. Spatial and temporal variations of groundwater quality of Qazvin plain. *Iran. Water Res. J.* **2011**, *5*, 41–52.
41. Singh, S.K.; Singh, C.K.; Mukherjee, S. Impact of land-use and land cover change of groundwater quality in the lower Shiwalik hills: A remote sensing and GIS based approach. *Cent. Eur. J. Geosci.* **2010**, *2*, 124–131. [[CrossRef](#)]
42. Farrag, A.A.; Megahed, H.A.; Darwish, M.H. Remote sensing, GIS and chemical analysis for assessment of environmental impacts on rising of groundwater around Kima Company, Aswan, Egypt. *Bull. Natl. Res. Cent.* **2019**, *43*, 14. [[CrossRef](#)]
43. Hussien, H.M.; Kehew, A.E.; Aggour, T.; Korany, E.; Abotalib, A.Z.; Hassanein, A.; Morsy, S. An integrated approach for identification of potential aquifer zones in structurally controlled terrain: Wadi Qena basin, Egypt. *Catena* **2017**, *149*, 73–85. [[CrossRef](#)]
44. Abotalib, A.Z.; Heggy, E. Groundwater mounding in fractured fossil aquifers in the Saharan–Arabian desert. In Proceedings of the Conference of the Arabian Journal of Geosciences, Sousse, Tunisia, 25–28 November 2019; Springer: Cham, Switzerland, 2019; pp. 359–362. [[CrossRef](#)]
45. Elsheikh, A.E. Mitigation of groundwater level deterioration of the Nubian Sandstone aquifer in Farafra Oasis, Western Desert, Egypt. *Environ. Earth Sci.* **2015**, *74*, 2351–2367. [[CrossRef](#)]
46. Ebraheem, A.; Riad, S.; Wycisk, P.; Seif El-Nasr, A. Simulation of impact of present and future groundwater extraction from the non-replenished Nubian Sandstone Aquifer in southwest Egypt. *Environ. Geol.* **2002**, *43*, 188–196. [[CrossRef](#)]
47. Powell, O.; Fensham, R. The history and fate of the Nubian Sandstone Aquifer springs in the oasis depressions of the Western Desert, Egypt. *Hydrogeol. J.* **2016**, *24*, 395–406. [[CrossRef](#)]
48. RIGW. *Hydrogeological Map of Egypt*, 1st ed.; Scale 1:2,000,000; Research Institute for Groundwater, Egyptian Ministry of Public Works and Water Resources: Cairo, Egypt, 2016.
49. Abotalib, A.Z.; Heggy, E.; El Bastawesy, M.; Ismail, E.; Gad, A.; Attwa, M. Groundwater mounding: A diagnostic feature for mapping aquifer connectivity in hyper-arid deserts. *Sci. Total Environ.* **2021**, *801*, 149760. [[CrossRef](#)]
50. Abotalib, A.Z.; Sultan, M.; Elkadiri, R. Groundwater processes in Saharan Africa: Implications for landscape evolution in arid environments. *Earth-Sci. Rev.* **2016**, *156*, 108–136. [[CrossRef](#)]

51. Sahour, H.; Sultan, M.; Abdellatif, B.; Emil, M.; Abotalib, A.Z.; Abdelmohsen, K.; Vazifedan, M.; Mohammad, A.T.; Hassan, S.M.; Metwalli, M.R.; et al. Identification of shallow groundwater in arid lands using multi-sensor remote sensing data and machine learning algorithms. *J. Hydrol.* **2022**, *614*, 128509. [[CrossRef](#)]
52. Sturchio, N.C.; Du, X.; Purtschert, R.; Lehmann, B.E.; Sultan, M.; Patterson, L.J.; Lu, Z.T.; Müller, P.; Bigler, T.; Bailey, K.; et al. One million year old groundwater in the Sahara revealed by krypton-81 and chlorine-36. *Geophys. Res. Lett.* **2004**, *31*. [[CrossRef](#)]
53. Khalil, M.M.; Tokunaga, T.; Heggy, E.; Abotalib, A.Z. Groundwater mixing in shallow aquifers stressed by land cover/land use changes under hyper-arid conditions. *J. Hydrol.* **2021**, *598*, 126245. [[CrossRef](#)]
54. Hu, K.; Huang, Y.; Li, H.; Li, B.; Chen, D.; White, R.E. Spatial variability of shallow groundwater level, electrical conductivity, and nitrate concentration, and risk assessment of nitrate contamination in the North China Plain. *Environ. Int. J.* **2005**, *31*, 896–903. [[CrossRef](#)]
55. Bucene, L.C.; Zimback, C.R.L. Comparison of methods of interpolation and spatial analysis of pH data in Botucatu-SP. *IRRIGA* **2003**, *8*, 21–28. [[CrossRef](#)]
56. Osati, K.H.; Salajegheh, A.; Arekhi, S. Spatial variability of nitrate in groundwater using geostatistics (Case study: Kurdan plain). *J. Range Watershed Manag.* **2012**, *65*, 461–472.
57. Wilcox, L.V. *Classification and Use of Irrigation Water*; U.S. Department of Agriculture, Salinity Laboratory: Washington, DC, USA, 1955; Volume 969.
58. Schoeller, H. Geochemie des eaux souterraines. *Rev. Inst. Fr. Pet.* **1962**, *10*, 230–244.
59. Lokhande, P.B.; Mujawar, H.A. Graphic interpretation and assessment of water quality in the Savitri River Basin. *Int. J. Sci. Eng. Res.* **2016**, *7*, 1113–1123.
60. Balakrishnan, P.; Saleem, A.; Mallikarjun, N.D. Groundwater quality mapping using GIS: A case study of Gulbarga city, Karnataka, India. *Afr. J. Environ. Sci. Technol.* **2011**, *5*, 69–108. [[CrossRef](#)]
61. WHO. *Guidelines for Drinking-Water Quality World Health Organization*, 4th ed.; World Health Organization: Geneva, Switzerland, 2011; pp. 219–244.
62. Khangembam, S.; Kshetrimayum, K.S. Evaluation of hydrogeochemical controlling factors and water quality index of water resources of the Barak valley of Assam. Northeast India. *Ground Sustain. Dev.* **2019**, *8*, 541–553. [[CrossRef](#)]
63. Wu, J.; Zhao, Y.; Qi, H.; Zhao, X.; Yang, T.; Du, Y.; Zhang, H.; Wei, Z. Identifying the key factors that affect the formation of humic substance during different materials composting. *Bioresour. Technol.* **2017**, *244*, 1193–1196. [[CrossRef](#)]
64. ESRI. *ArcGIS 10.3 Desktop*; Environmental Systems Research Institute, Inc.: Redlands, CA, USA, 2015; pp. 1–232.
65. ENVI. *Software Package Ver. 5.3., ENVI User's Guide*; Research Systems Inc.: Norwalk, CT, USA, 2018; p. 1128.
66. Joshi, V.U.; Nagare, V. Land-use change detection along the Pravara river basin in Maharashtra, using remote sensing and GIS techniques. *AGD Landsc. Environ.* **2009**, *3*, 71–86.
67. Deshmukh, K.K. Assessment of groundwater quality in Sangamner area for sustainable agricultural water use planning. *Int. J. Chem. Sci.* **2011**, *9*, 1486–1500.
68. Deshmukh, R.A.; Jagtap, S.; Mandal, M.K.; Mandal, S.K. Purification, biochemical characterization and structural modelling of alkali-stable β -1, 4-xylan xylanohydrolase from *Aspergillus fumigatus* R1 isolated from soil. *BMC Biotechnol.* **2016**, *16*, 11. [[CrossRef](#)]
69. Dams, J.; Wodeamlak, S.T.; Batelaan, O. Predicting land-use change and its impact on the groundwater systems of the Kleine Nete catchment, Belgium. *Hydrol. Earth Syst. Sci.* **2008**, *12*, 1369–1385. [[CrossRef](#)]
70. Tang, Z.; Engel, B.A.; Pijanowski, B.C.; Lim, K.J. Forecasting land-use change and its environmental impact at a watershed scale. *J. Environ. Manag.* **2005**, *76*, 35–45. [[CrossRef](#)]
71. Bhaduri, B.; Harbor, J.; Engel, B.; Grove, M. Assessing watershed-scale, long-term hydrologic impacts of land-use change using a GIS-NPS model. *Environ. Manag.* **2000**, *26*, 643–658. [[CrossRef](#)]
72. Metwaly, M.M.; AbdelRahman, M.A.E.; Abdellatif, B. Heavy metals and micronutrients assessment in soil and groundwater using geospatial analyses under agricultural exploitation in dry areas. *Acta Geophys.* **2022**. Available online: <https://link.springer.com/article/10.1007/s11600-022-00979-1> (accessed on 1 January 2023). [[CrossRef](#)]

Disclaimer/Publisher's Note: The statements, opinions and data contained in all publications are solely those of the individual author(s) and contributor(s) and not of MDPI and/or the editor(s). MDPI and/or the editor(s) disclaim responsibility for any injury to people or property resulting from any ideas, methods, instructions or products referred to in the content.